*Desalination and Water Treatment*
www.deswater.com

doi:10.5004/dwt.2018.22038

106 (2018) 165–176
February

# Adsorptive and thermodynamic properties derived from different synthetic zeolite – groundwater ammonium species molar ratios

Miroslav Kukučka[a], Nikoleta Kukučka Stojanović[a,*], Željko Tomić[b], Danilo Furundžić[c]

[a]*Envirotech d.o.o., SterijePopovića 42, 23300 Kikinda, Serbia, Tel. +381230439200, email: miroslav@envirotech.rs (M. Kukučka), nikol@envirotech.rs (N.K. Stojanović)*
[b]*Institute for Work Safety, 21000 Novi Sad, Školska 3, Serbia, Tel. +38121421700, email: zeljko.tomic@institut.co.rs*
[c]*Public enterprise "Kikinda", Iđoški put 4, 23300 Kikinda, Serbia, Tel. +381230422760, email: dfurundzic@gmail.com*

Received 2 October 2017; Accepted 12 February 2018

**ABSTRACT**

In order to investigate potential effect of synthetic zeolite and groundwater ammonium species molar ratios(MCQ) on the sorption and thermodynamic parameters, batch experiments of groundwater ammonium ion (AMI) adsorption were conducted using synthetic zeolite CR-100 (CR). Commercial CR adsorbent, and CR after the equilibrium at the lowest MCQ were characterized by Fourier transform infrared (FTIR) spectroscopy. Adsorption studies at three temperatures were carried out to evaluate CR potential for AMI removal. Results showed that AMI removal efficiency (η) decreased (279 K > 289 K > 299 K) at higher MCQ values, and to opposite increased (279 K < 289 K < 299 K) at lower MCQ, where the highest η was 85.11% at 279 K. Isotherm curve shapes showed that investigated ammonium ion adsorption on CR is a multi-layer process. The AMI adsorption results fitted the Freundlich isotherm model very well, with CR adsorption capacity from 4.85 mg/L (279 K) to 11.38 mg/L (299 K), and the sorption process can be described by a pseudo-second order kinetic model. Obtained standard free energy values were negative at all experimental temperatures and indicated that ammonium sorption process on CR was spontaneous with physical characteristics. Adsorption process was found to be slightly exothermic and spontaneous when MCQ was low, and exothermic and non-spontaneous in the conditions of high MCQ.

*Keywords:* Ammonium ion; Synthetic zeolite; Molar concentration quotient; Enthalpy; Entropy

## 1. Introduction

A considerable number of citizens in the Province of Vojvodina, Northern part of Serbia, are supplied with a drinking water that is consisted of elevated, geologically originated, ammonium ion (AMI) with concentration four times higher than maximum tolerable concentration (MTC), regarding to legislation proposal [1]. Distribution of drinking water with ammonium ion concentration below MTC to the public is actual, long time problem, and needs attention of the scientists.

There are many sorption methods for ammonium ion removal from natural water [2,3] and wastewater [4]. Membrane separation techniques are also widely used for elimination of ammonium ions from aquatic solutions [5,6]. Adsorption of ammonium ions onto natural [7,8] and synthetic zeolites [9,10] were presented in many studies.

Zeolites are hydrated silicates of aluminium, alkaline and alkaline earth metals. Primary building block of zeolites framework is tetrahedron. An aluminium or silicon atom and four oxygen atoms in vertexes occupy center of tetrahedron. Many tetrahedrons build the zeolite framework. Consequence of the substitution of $Si^{4+}$ with $Al^{3+}$ ions is appearance of negatively charged framework with the positive counter ions of monovalent or divalent cations, including water molecules [11]. The existing voids are positioned between the tetrahedrons, in large cavities with aqueous bridges between the framework and exchangeable

*Corresponding author.

ions. The zeolite voids represent porous structure suitable for adsorption of different chemical species.

Adsorption studies of different adsorbates vs. adsorbents systems are usually based on determination of adsorbent equilibrium adsorption capacities in function of adsorbate equilibrium adsorption concentrations [12,13]. Establishment of these physical units' dependencies and their incorporation into different types of adsorption isotherm model equations, enables significant isotherm constants calculation [14,15]. These constants are related to sorption energy and heat, adsorption-desorption ratio, adsorbent maximum sorption capacity, nature of sorption, and other essential data regarding adsorbent-adsorbate interactions. The best following of experimental sorption data with different adsorption isotherm models by linear and nonlinear regression determination, indicates the best fitted type of mathematical sorption model [16].

Sorption thermodynamics and kinetics of different species on wide spectrum of adsorbents were favored subject of scientist with an especial attention to investigation of temperature and adsorbent mass effects on adsorption capacity [17,18]. Increase in temperature, as a crucial sorption parameter, can result in decline [19,20] or may enhance sorption capacity [21].

Adsorption capacity decreases [22] or increases[23] with the rise of adsorbent dosage, depending on the nature of sorption system and applied physical conditions.

Besides, aquatic ammonium ions adsorption on different natural [24] and synthetic [25] materials was widely investigated. Thermodynamic parameters such as a change in free energy, enthalpy and entropy were investigated for a long time [26]. Evaluation of spontaneous or unspontaneous adsorption mechanism nature particularly depends on different adsorbent constitution and species solution physicochemical properties [27,28].

Kim found a higher adsorption at a lower adsorbate/adsorbent ratio [29]. Influence of adsorbent concentration at different temperatures on thermodynamic parameters value in the identical sorption system, which should be significant to spontaneity process nature changes, was poorly investigated or not clearly explained [30].

The scope of these investigations was to conclude potential effect of molar ratio of synthetic zeolite and groundwater ammonium species on the thermodynamic and kinetic parameters, and sorption process spontaneity, as well.

## 2. Materials and methods

The origin of ammonium ion used for investigation of zeolite sorption and thermodynamic characteristics was natural groundwater located in City of Kikinda, Northern Vojvodina (Serbia) (Latitude 45.827284; Longitude 20.461517). The main constituents of this water besides ammonium ion were high contents of dissolved natural organic matter and arsenic, sodium and bicarbonate ions, along with consequentially high pH of 8.3. Additionally, groundwater was intensively yellow colored with distinct low hardness [31].

Groundwater ammonium ion adsorption batch experiments were investigated using synthetic zeolite Crystal Right, type CR-100 *(CR)* [32], which chemical and physical properties were taken from manufacturer's data sheet. Molecular weight of *CR*'s white-light gray crystals is 1,523 g/mol and 1,109 g/mol for hydrated and anhydrous form, respectively. Specific gravity of the synthetic zeolite at 295 K is 0.686 kg/m$^3$. CR particle size range was from 0.3 to 2.4 mm. CR is a sodium aluminium-silicate with Si : Al ratio of 3.2 [33]. Investigated zeolite elemental analysis was examined in the previous research by energy dispersive spectroscopy (EDS) [34]. Results show that zeolite is consisted of 42.83% of Si, 30.06% of O, 13.20% of Al, 4% of Na and 9.92% of Ca. Specific surface area of CR was 147 m$^2$/g with average pore diameter of 14.71 nm [34].

CR samples were crushed and sieved to a size range of 0.1 to 0.2 mm. CR was washed to remove water soluble residues and other undesirable material, and dried in an oven at 180±5°C for 8 h. Batch experiments were conducted using different masses of adsorbent dispersed in 100 mL of investigated groundwater. Initial groundwater ammonium ion nitrogen ($NH_4^+$-N)concentration ($C_0$) was 2.14 mg/L (0.1529 mmol/L). CR adsorbent concentrations ($C_{adt}$) in g/L, used in experiments were 0.1, 0.4, 0.8, 1.2, 1.5, 1.8, 2.0, 2.8 and 3.5 g/L. For kinetic studies, experiments were conducted with 100 mL of groundwater and 0.8 g/L of CR at different contact time (t) of 10 to 120 min. The bottles were placed on Gallenkamp orbital shaker at 279, 289 and 299 K and speed of 200 rpm in all the experiments.

The residual concentrations of ammonium ion were determined by samples analysis after centrifugation in the laboratory with standard colorimetric method using the Nessler solution. All experiments were repeated three times.

Ammonium ion uptake was calculated using the following equation:

$$q_{e(t)} = \frac{C_0 - C}{C_{adt}} \tag{1}$$

where $q_e$ (mg/g) and $q_t$ (mg/g) represent amount of equilibrium ammonium nitrogen adsorbed on CR, in the batch and kinetic experiments, respectively. *C* (mg/L) represents equilibrium ammonium nitrogen concentration.

The removal efficiency of groundwater AMI onto CR, η in %, was calculated using expression:

$$\eta = \frac{C_0 - C}{C_0} \cdot 100 \tag{2}$$

Dimensionless measure unit of molar concentrations quotient (MCQ) is defined as the ratio of CR and the initial AMI concentration, both in mmol/L, and was calculated as shown in Eq. (3).

$$MCQ = \frac{C_{adt}}{C_0} \tag{3}$$

MCQ is very significant for easier apperception of the adsorbent and the adsorbate relative contemporarily presence in solution, as well as, for elucidation of adsorption thermodynamic findings for the different $C_{adt}$.

Infrared absorption spectra were measured at room temperature on a FTIR spectrometer Thermo Nicolet Nexus 670, using DTGSdetector. 10 mg of sample was lyophilized, gently mixed with 300 mg of KBr powder and compressed into discs at a force of 17 kN for 5 min using a tablet presser.

## 3. Theoretical background

### 3.1. Equilibrium isotherm models

With the use of equilibrium ammonium concentrations and ammonium adsorbed per mass unit of adsorbent equilibrium experimental values, it is possible to calculate the constants of several adsorption isotherm models. Linear correlation coefficients ($R^2$) obtained by least squares method of each isotherm equation linearized plot indicate fitting level to experimentally obtained data. The goal of those operations was determination of adsorption nature, maximum zeolite uptake of ammonium ion, and indication of the basic thermodynamic process parameters.

The Langmuir`s monolayer adsorption model (LIM) enables calculation of monolayer adsorption capacity $q_m$ in mg/g, and constant $K_L$ related to binding energy, and is represented in Eq. (4) [35].

$$q_e = \frac{K_L \cdot q_m \cdot C}{1 + K_L \cdot C} \tag{4}$$

Linearization of Eq. (4), presented in Eq. (5) in the form of $1/q_e$ vs. $1/C$ enables calculation of $q_m$ and $K_L$ from the slope and intercept, respectively.

$$\frac{1}{q_e} = \left(\frac{1}{K_L \cdot q_m}\right) \cdot \frac{1}{C} + \frac{1}{q_m} \tag{5}$$

The Freundlich empirical sorption isotherm model (FIM), suitable for non-ideal systems, involved intramolecular interactions onto heterogenic adsorbent surface. This adsorption model is presented in Eq. (6) [36].

$$q_e = K_F \cdot C^{1/n_F} \tag{6}$$

Heterogeneity factor $n_F$ indicates whether the adsorption process is linear, chemical or physical for $n_F = 1$, $n_F < 1$ and $n_F > 1$, respectively. In the same time, the values of $1/n_F < 1$ indicate a normal Langmuir isotherm and opposite to that, $1/n_F > 1$ values hint a cooperative adsorption [37]. Constant $K_F$ (L/g) is related to adsorption capacity, and according to Eq. (7) [38], enables calculation of the Freundlich maximum adsorption capacity ($Q_F$) in mg/g.

$$Q_F = K_F \cdot C_0^{1/n_F} \tag{7}$$

Linearized form of Eq. (6), shown in Eq. (8), expressed as a plot log ($q_e$) vs. log ($C$), enables calculation of the Freundlich constants $1/n_F$ and $K_F$, as a slope and antilogarithm of the intercept, respectively.

$$\log(q_e) = \log(K_F) + \frac{1}{n_F} \cdot \log(C) \tag{8}$$

Assumptions of the Temkin isotherm model (TIM) are adsorbent-adsorbate interactions on the surfaces, and consequently,the heat of adsorption linear decrease with the sorption coverage, rather than logarithmic. This sorption model alludes chemical sorption with uniformed binding energy [39]. The Temkin isotherm equation is given in Eq. (9).

$$q_e = \frac{R \cdot T}{b_T} \cdot \ln(K_T \cdot C) \tag{9}$$

From the plot $q_e$ vs. ln($C$) based on the linearized form of Eq. (9), Temkin`s isotherm constant $K_T$ in L/g and heat of the adsorption $b_T$ (J/mol) can be calculated from the intercept and slope, respectively. TIM linear form is presented in Eq. (10) where parameter R (8.314 J/mol·K) is the ideal gas constant and T (K) is absolute temperature.

$$\ln(q_e) = \frac{R \cdot T}{b_T} \cdot \ln(K_T) + \frac{R \cdot T}{b_T} \cdot \ln(C) \tag{10}$$

The Dubinin-Radushkevitch isotherm model (DRI) assumes that characteristic of the sorption curve is related to the adsorbent porosity. The basis of the DRI is the theory of micro pores volume filling and adsorption potential theory of Polanyi [40]. DRI mathematical expression is presented in Eq. (11), which can be transformed in linearized form. Linear plot ln ($q_e$) vs. $\varepsilon^2$ enables calculation of DRI maximum sorption capacity $Q_D$ (mg/g) and constant $K_D$ related to the mean free energy of sorption in $mol^2/kJ^2$ from the intercept and slope, respectively. Linearized Eq. (11) is presented in Eq. (12).

$$q_e = Q_D \cdot EXP(-K_D \cdot \varepsilon^2) \tag{11}$$

$$\ln(q_e) = \ln(Q_D) - K_D \cdot \varepsilon^2 \tag{12}$$

Parameter ε can be calculated from Eq. (13).

$$\varepsilon = R \cdot T \cdot \ln\left[1 + \frac{1}{C}\right] \tag{13}$$

In addition, $K_D$ is the base for calculation of the mean free energy E (J/mol) of adsorption per molecule of adsorbate during the transfer from infinity of solution to the surface of the adsorbent, and is presented in Eq. (14).

$$E = \frac{1}{\sqrt{2 \cdot K_D}} \tag{14}$$

The Jovanovic isotherm model (JIM) contained the similar assumptions like the LIM, considering possibilities of some physical interactions between adsorbing and desorbing molecules [37,41]. This model leads to the relationship showed in Eq. (15).

$$q_e = Q_J \cdot (1 - e^{K_J \cdot C}) \tag{15}$$

JIM constant $K_J$ (L/g) and maximum adsorbate uptake $Q_J$ (mg/g) can be calculated from the slope and intercept of the linearized Eq.(15) linear dependence ln($q_e$) vs. C expressed in Eq. (16).

$$\ln(q_e) = \ln(Q_J) - K_J \cdot C \tag{16}$$

#### 3.1.1. Error analysis

Making different isotherm models linear plots coefficient of determination ($R^2$) values comparison, as usual

method for determination of experimental isotherm data fitting level does not represents the errors in the isotherm curves. $R^2$ values based on the isotherm equations linearized forms are not certain enough to give good fit of theoretical values of equilibrium adsorption capacity ($q_{e,cal}$) in mg/g to experimental data. Besides linear regression, non-linear regressions are very useful for isotherm models and experimental data commutual fite valuation. The chi-square ($\chi^2$) test [16,42], Eq. (17), and residual root mean square error (RMSE) [43], Eq. (18), were used to compare experimental and theoretical values of equilibrium adsorption capacity. In both Eq. (17) and Eq. (18) symbol $p$ is the number of observations in the experimental isotherm.

$$\chi^2 = \sum_{i=1}^{p} \frac{(q_{e(i)} - q_{e,cal(i)})^2}{q_{e,cal(i)}} \tag{17}$$

$$RMSE = \sqrt{\frac{1}{n-2} \cdot \sum_{i=1}^{p} (q_{e(i)} - q_{e,cal(i)})^2} \tag{18}$$

For both, $\chi^2$ and RMSE calculated values, as smaller number is obtained, the better is fitting of the assigned isotherm model to the experimental data.

### 3.2. Adsorption thermodynamics

Adsorption processes thermodynamic analysis have been conducted at different temperatures, first of all by calculation of standard free Gibbs energy based on the equation [44–46]:

$$\Delta G^0 = -R \cdot T \cdot \ln(K_{ad}) \tag{19}$$

where $\Delta G^0$ is change of the Gibbs free energy (kJ/mol), $R$ (8.314 J/mol·K) is the molar gas constant, $T$ is absolute temperature in K, and $K_{ad}$ is apparent adsorption equilibrium constant [47] expressed by Eq. (20):

$$K_{ad} = C_0 / C \tag{20}$$

Enthalpy and entropy were calculated using Gibbs free energy thermodynamic relation. At the base of essential thermodynamic lows, relation between Gibbs free energy, enthalpy and entropy was calculated as shown in expression:

$$\Delta G^0 = \Delta H^0 - T \cdot \Delta S^0 \tag{21}$$

where $\Delta H^0$ is enthalpy changes (kJ/mol) and $\Delta S^0$ entropy changes (kJ/mol).

Modification of Eq. (6) including incorporation of Eq. (4) [20] created expression:

$$\ln K_{ad} = \frac{\Delta S^0}{R} - \frac{\Delta H^0}{RT} \tag{22}$$

Linear dependence of van`t Hoff plots ln $K_{ad}$ vs. $1/T$ gives a possibility for calculation of enthalpy and entropy change values from the slope and the intercept, respectively. Adsorption process spontaneity [48] can be examined from the Gibbs free energy value. Negative value of $\Delta G^0$ indicates spontaneous adsorption process, when adsorption system uses its own energy for physicochemical interactions.

### 3.3. Adsorption kinetics modeling

The kinetics of groundwater ammonium ion is an important characteristic for understanding the sorption efficiency and usage of CR for groundwater treatment feasibility. Hence, the kinetics of ammonium removal was measured as a function of ammonium ion and temperature. The sorption data were simulated by both, pseudo-first [49,50], and pseudo-second kinetic models [51,52], which are expressed by Eq. (23), and Eq. (24), respectively:

$$\ln(q_e - q_t) = \ln q_e - k_1 \cdot t \tag{23}$$

where $k_1$ is Lagergren's adsorption rate constant of the first-order (g/mg·min), and $q_t$ (mg/g) is amount of adsorbed *AMI* on *CR* in defined time. The values of $q_e$ and $k_1$ were calculated from the intercept and slope of the plot $ln\ (q_e - q_t)$ vs. $t$.

$$\frac{t}{q_t} = \frac{1}{k_2 \cdot q_e^2} + \frac{t}{q_e} \tag{24}$$

The $k_2$ is the rate constant of the second-order adsorption in g/mg·min. The values of $k_2$ and $q_e$ were determined from the intercept and slope of the plot of $t/q_t$ vs. $t$. Reciprocal of the intercept from Eq. (24) can be regarded as the initial sorption rate ($h$) in mg/g·min [53], as $q_t/t \to 0$, and is presented in Eq. (25).

$$h = k_2 \cdot q_e^2 \tag{25}$$

## 4. Results and discussion

### 4.1. Ammonium ion removal efficiency

Groundwater ammonium ion removal efficiency by synthetic zeolite CR was determined during the experiments and presented in Fig. 1. AMI removal efficiency increases, in general,with CR concentration. At lower $C_{adt}$ till 1.2 g/L, η was sharply increased in order 279 K < 289 K < 299 K, but at higher CR concentrations opposite order was found, 279 K > 289 K > 299 K, which was probably a consequence of adsorptive forces decay between the ammonium species and the CR surface active sites with the temperature [54]. Effects of higher $C_{adt}$ accompanied by temperature increase are not in accordance with the earlier findings that room temperature is confining factor for η progress or decay [55].

### 4.2. Adsorption isotherm modeling

Effects of different temperature on groundwater ammonium adsorption process under batch experimental conditions were studied. Obtained values of equilibrium ammonium ion concentrations and $q_e$ (Eq. (1)) were imported to LIM, FIM, TIM, DRI, and JIM linearized equations, to test the accuracy of the isotherm models in order to represent the experimental data through calculation of the coefficient of determination. FIM, TIM, DRI, and JIM linear regression plots at 279 K, 289 K,

and 299 K are shown in Fig. 2. Isotherm constants calculated from linear plots (Fig. 2) are given in Table 1.

Langmuir isotherms experimental linear plots at all three investigated temperatures possessed negative intercepts which disabled calculation of LIM constants $K_L$ and $q_m$ [Eq. (5)]. These results suggested that adsorption system zeolite CR-groundwater ammonium ion does not follow assumptions of the Langmuir approach. Impossibility of the calculation of the constants related to the surface binding energy and monolayer coverage, indicates the inadequacy of the LIM to describe the adsorption process.

Equilibrium data analyzed using the Freundlich model (Fig. 2a), show increase of both FIM constants $K_F$ and $1/n_F$ with increase of temperature, indicating adsorption capacity rise. The values of $1/n_F$, as a function of adsorption strength, were higher than unity which hint a cooperative adsorption process, whereas $n_F$ values found below one are suggesting chemical adsorption process. At the lowest temperature of 279 K value of $1/n_F$ was near unity indicating almost linear adsorption isotherm, suggesting that competition for ammonium ions between liquid and solid phase was the same or increasing at the same rate. Constant $1/n_F$ is related to the distribution of the site energy, and the lower the values are, more heterogeneous site distribution is indicative [56]. Extent of the Freundlich maximum sorption capacity increased with an increase in temperature, suggesting endothermic process. The increase in sorption capacity at higher temperatures may be attributed to more intensive multilayer bonding to the adsorbent active sites.

According to the linearized TIM expression (Fig. 2b) estimated constant $b_T$ values were positive, between 0.58 and 1.07 kJ/mol (Table 1), and indicate exothermic nature of the process [57]. Temkin binding constant and heat of sorp-

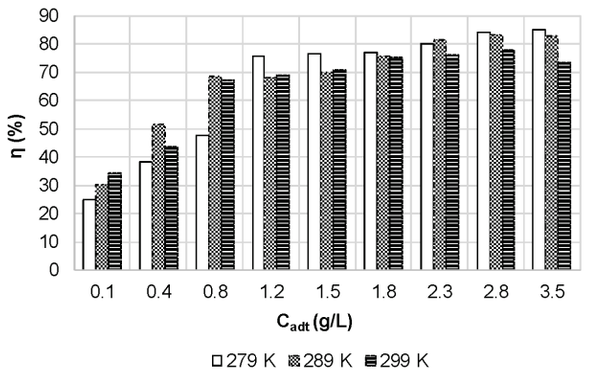


Fig. 1. Effect of zeolite CR concentration on groundwater ammonium ions removal efficiency at different temperatures.

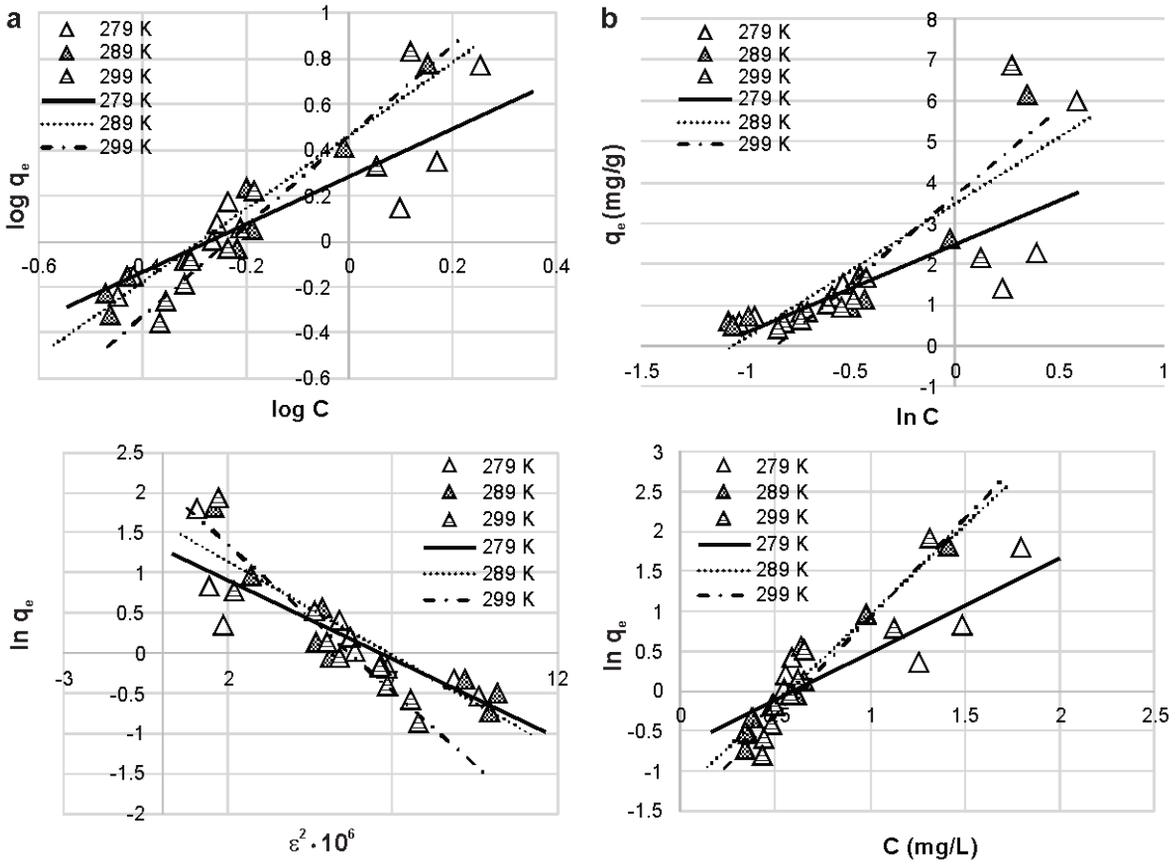


Fig. 2. Linear plots of Freundlich (a), Temkin (b), Dubinin-Radushkevitch (c), and Jovanovic (d) isotherms of groundwater $NH_4^+$-N on synthetic zeolite CR at different temperatures.

Table 1
Comparison of the isotherm parameters and linear regression coefficients of determination

| Isotherm model | Parameters | Temperature (K) | | |
|---|---|---|---|---|
| | | 279 | 289 | 299 |
| Freundlich (Eq. (8)) | $K_F$ (L/g) | 1.938 | 2.897 | 2.799 |
| | $1/n_F$ | 1.043 | 1.604 | 2.023 |
| | $n_F$ | 0.958 | 0.623 | 0.494 |
| | $Q_F$ (mg/g) | 4.815 | 8.995 | 11.376 |
| | $R^2$ | 0.8032 | 0.9356 | 0.8404 |
| Temkin (Eq. (10)) | $K_T$ (L/g) | 3.189 | 2.897 | 2.266 |
| | $b_T$ (J/mol) | 1,067.89 | 734.13 | 554.42 |
| | $R^2$ | 0.6078 | 0.7802 | 0.7277 |
| Dubinin-Radushkevitch (Eq. (12)) | $K_D$ (mol²/kJ²) | 2E-07 | 2E-07 | 4E-07 |
| | $Q_D$ (mg/g) | 3.634 | 5.015 | 7.988 |
| | $E$ (J/mol) | 1,581 | 1,581 | 1,118 |
| | $R^2$ | 0.7596 | 0.8344 | 0.8160 |
| Jovanovic (Eq. (16)) | $K_J$ (L/g) | 1.187 | 2.230 | 2.495 |
| | $Q_J$ (mg/g) | 0.499 | 0.285 | 0.204 |
| | $R^2$ | 0.8222 | 0.9486 | 0.8387 |

tion decreased with the temperature increase, confirmed that sorption was not favorable at high temperatures and the process was exothermic.

DRI constants $K_D$ and maximum adsorption capacity showed increasing trend with the temperature increase (Fig. 2c). At the same instant, the mean free sorption energies calculated from Eq. (14) expressed decreasing tendency. Obtained E values were higher than 1 kJ/mole, and gave information that investigated process was physisorption [57].

Although the Jovanovic isotherm model is in essential postulate similar to the Langmuir model, obtained data fitted to experimental data (Fig. 2d), and it was possible to calculate JIM constants from Eq. (16). Obviously JIM expression referred to limited monolayer part of adsorbed ammonium ions, taking into account their surface binding vibrations. Adsorbate maximum adsorption capacities onto CR surface were approximated to localized sorption without lateral interactions, and decreased with the temperature increase, indicating physical sorption process.

Linear regression coefficients of determination values for all four applied isotherm models depended on temperature and were distributed in next order: $R^2$(289 K) > $R^2$(299 K) > $R^2$(279 K). Linear fitting of the sorption experimental data to different adsorption isotherm models were variable depending on the temperature as follows: at 279 K and 289 K were $R^2$ (JIM) > $R^2$ (FIM) > $R^2$ (DRI > $R^2$ (TIM), and at 299 K were $R^2$ (FIM) > $R^2$ (JIM) > $R^2$ (DRI > $R^2$ (TIM). Maximum adsorption capacities measure ratio descended in the next order FIM > DRI > JIM, at all investigated temperatures.

Besides described, nonlinear fitting of FIM, TIM, DRI, and JIM to experimental data were applied.

Experimental adsorption isotherms and theoretical prediction of equilibrium adsorption capacities for FIM, TIM, DRI, and JIM at 279 K, 289 K, and 299 K are shown in Fig. 3.

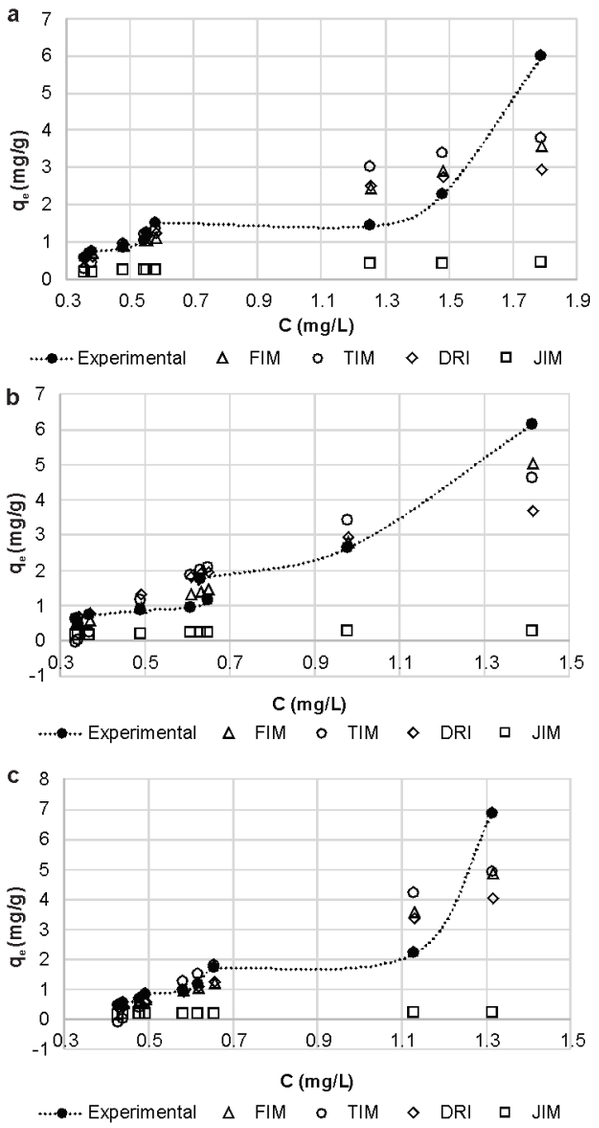


Fig. 3. Freundlich, Temkin, Dubinin-Radushkevitch, and Jovanovic groundwater ammonium ions adsorption isotherms on synthetic zeolite CR-100 at a. 279 K, b. 289 K, and c. 299 K.

All three experimental isotherm curve shapes, presented in Fig. 3, are showing that investigated ammonium ion adsorption on *CR* is multi-layer process [58]. In the zone of AMI equilibrium concentrations smaller than 0.65 mg/L (corresponding to the higher MCQ values), adsorption capacities decreased with an increase of temperature as similarly found earlier [30]. Opposite to that, higher temperatures contributed to enormous progress in $q_e$ values contributing to the multi-layer zone existence. Preliminary was reported for some other adsorbents [59,60] that multilayer adsorption process area needs additional energy at higher temperatures. Temperature influence on adsorbate solubility was discernible, having as a consequence different behavior of the investigated synthetic zeolite in the

same ammonium solution. Adsorbate solubility increased with temperature at the higher $C_{adt}$ values thus declining adsorbed ammonium amount. Lower *CR* concentrations contributed to predominant adsorbate solubility decrease for the identical temperatures. Additionally, adsorbed and diluted ammonium interface interactions, at adsorbent surface, were probably result of competitiveness of a lot of adsorbate species for limited zeolite active sites. Similar phenomena have been found recently [61], but for the different sorption systems.

Nonlinear fitting of presented isotherm models plots to experimental isotherm plot (Fig. 2), at different temperatures were employed in this study through error analysis evaluation. Results of $\chi^2$ [Eq. (17)] and *RMSE* [Eq. (18)] calculations for investigated isotherm models are presented in Table 2.

In opposite to findings obtained from linear correlation coefficients that Jovanovic isotherm model fitted the best to the experimental data at temperatures of 279 K and 289 K, results of error analysis showed contradicting observations. Particularly, *RMSE* and $\chi^2$ indicated that the best nonlinear fit belongs to the Freundlich isotherm model assumptions at all three investigated temperatures. Opposite to that, the *JIM* showed the worst correlation of experimental and calculated $q_e$ values. Error values of the Temkin and the Dubinin-Radushkevitch models were close and could describe the subject of adsorption process with less accuracy than *FIM*. Especially, obtained thermodynamic data of *TIM* and *DRI* indicated significant conclusion about nature of the process, as showed earlier [62].

### 4.3. Adsorption thermodynamics

Gibbs free energy changes were calculated using Eqs. (19) and (20), and their dependence on *CR* equilibrium ammonium capacity are shown in Fig. 4.

Similar coherence between $C_{adt}$, i.e. *CR* equilibrium capacity and temperature changing can also be found as a Gibbs free energy variations (Fig. 4). Particularly, adsorbate solubility increase was followed with $\Delta G^0$ descending, opposite to conditions of reduced ammonium ion solubility, at the same temperature regime, when the $\Delta G^0$ was raised.

Relative values of Gibbs free energy were increased across the adsorption process more than five times (Fig. 4). It can be seen that more favorable adsorption occurred in the area of high zeolite adsorption capacity when $\Delta G^0$ was the highest and decreased with temperature. Therefore, $\Delta G^0$ values were as lower as ammonium uptake was smaller, and increased with temperature. Obtained standard free energy values were negative at all experimental temperatures and indicated that ammonium sorption process on *CR* was spontaneous with physical characteristics [63].

Effects of the different zeolite concentrations, as well as solid/liquid molar concentration quotient on changes of apparent equilibrium constant and ammonium removal efficiency areshown in Table 3.

$\Delta H^0$ and $\Delta S^0$changes of investigated adsorption process in the dependence of *MCQ* (Fig. 5a) were determined from the slope and intercept of the plots $ln\ (K_{ad})$ vs. $1/T$ (Eq. (22)) shown in Table 3. Both $\Delta H^0$ and $\Delta S^0$were considered in order to determine Gibbs free energy of the process. Influence of different $C_{adt}$ values on $\Delta G^0$ changes at three investigated temperatures are presented in Fig. 5b.

Different $C_{adt}$, i.e., *MCQ* values induced diverse thermodynamic performance estimation of investigated adsorption process (Fig. 5). *CR* zeolite concentration increase showed tendency of enthalpy slow increase and, in the same time, some more efficient trend of entropy decrease (Fig. 5a). To that, both $\Delta H^0$ and $\Delta S^0$ have changed number signs, from minus to plus and vice versa, respectively, assigning availability of nuance of thermodynamic properties in the same adsorption system. Similar ammonia adsorption entropy change trends were obtained previously [64], but without changing of the sign. The $\Delta S^0$ positive and negative values suggest, respectively, increased and decreased randomness at the zeolite/ammonium ion solution interface during the sorption process [30,65]. Positive values of standard entropy changes corresponded to an increase in the degree of freedom of the adsorbed ammonium ions. In contrast, enthalpy change values were negative in the area of low $C_{adt}$ values and showed exothermic phase of ammonium adsorption process [66]. When the CR concentration increased, $\Delta H^0$ became positive, estimating slightly endothermic process nature.

Significant changes in the slopes of Van`t Hoff plots (Table 3) as well as trends of relative Gibbs energy vs. temperature (Fig. 5b) obtrude a premise that investigated pro-

Table 2
Four isotherm models at different temperatures error analysis results comparison

| Isotherm model | Parameters | Temperature (K) | | |
|---|---|---|---|---|
| | | 279 | 289 | 299 |
| Freundlich | RMSE | 1.0421 | 0.4772 | 0.9490 |
| | $\chi^2$ | 2.4285 | 0.5509 | 1.6197 |
| Temkin | RMSE | 1.1239 | 0.8993 | 1.1242 |
| | $\chi^2$ | 3.0594 | 3.9064 | 3.8346 |
| Dubinin-Radushkevitch | RMSE | 1.2437 | 1.0574 | 1.1883 |
| | $\chi^2$ | 3.8210 | 2.6750 | 2.8309 |
| Jovanovic | RMSE | 2.3739 | 2.5289 | 2.7590 |
| | $\chi^2$ | 98.8806 | 171.9198 | 277.8951 |

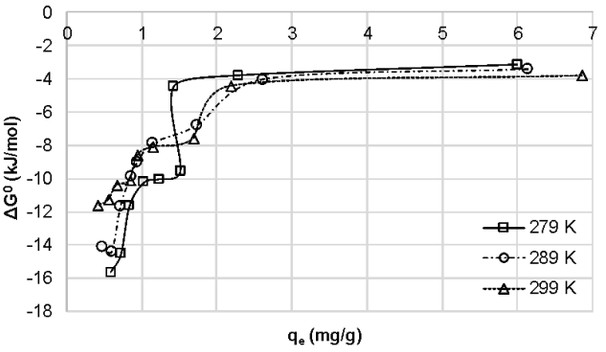


Fig. 4. Gibbs free energy changes dependence on ammonium uptake quantity at different temperatures.

Table 3
Dependence of CR concentration on van`t Hoff plot at different temperatures

| $C_{adt}$ (mmol/L) | MCQ | ln $K_{ad}$ | $1/T$ ($K^{-1}$) × $10^{-3}$ | Slope | Intercept | $R^2$ |
|---|---|---|---|---|---|---|
| 0.066 | 0.430 | 0.288 | 3.58 | –548.35 | 2.25 | 0.9986 |
| | | 0.361 | 3.46 | | | |
| | | 0.420 | 3.34 | | | |
| 0.263 | 1.718 | 0.480 | 3.58 | –388.62 | | |
| | | 0.519 | 3.46 | | 1.87 | 0.9875 |
| | | 0.573 | 3.34 | | | |
| 0.525 | 3.436 | 0.645 | 3.58 | | | |
| | | 1.040 | 3.46 | –1,981.10 | 7.79 | 0.8810 |
| | | 1.117 | 3.34 | | | |
| 0.788 | 5.155 | 1.412 | 3.58 | | | |
| | | 1.188 | 3.46 | 990.21 | –2.17 | 0.8006 |
| | | 1.177 | 3.34 | | | |
| 0.985 | 6.443 | 1.461 | 3.58 | | | |
| | | 1.322 | 3.46 | 940.15 | –1.92 | 0.9865 |
| | | 1.236 | 3.34 | | | |
| 1.182 | 7.732 | 1.480 | 3.58 | | | |
| | | 1.417 | 3.46 | 334.64 | 0.27 | 0.9047 |
| | | 1.401 | 3.34 | | | |
| 1.510 | 9.879 | 1.609 | 3.58 | | | |
| | | 1.579 | 3.46 | 744.89 | –1.04 | 0.8576 |
| | | 1.429 | 3.34 | | | |
| 1.838 | 12.027 | 1.833 | 3.58 | | | |
| | | 1.790 | 3.46 | 1,329.70 | –2.89 | 0.8325 |
| | | 1.511 | 3.34 | | | |
| 2.298 | 15.034 | 1.905 | 3.58 | | | |
| | | 1.770 | 3.46 | 2,383.00 | –6.58 | 0.9023 |
| | | 1.330 | 3.34 | | | |

cess spontaneity is exactly proportional to $C_{adt}$. Gibbs free energy changes are indicative for comparison of relative energies of different adsorption phases regard to ammonium uptake capacities.

Periodical changes of $\Delta H^0$ and $\Delta S^0$ (Fig. 5a) with the MCQ increase also confirm existence of three step AMI sorption process on CR found recently [67]: Initial i.e. lowest MCQ values represent the CR exhausting area. Thus, cross section of positive $\Delta S^0$ and negative $\Delta H^0$ near MCQ of 4.8 probably means launching of the third spontaneous adsorption step that occurrs in second sorption layer, where $q_e$ was the highest (Fig. 3). Aggregation of residual binding sites possibly started in this area [68]. The overlapping point of the negative $\Delta S^0$ and positive $\Delta H^0$ at ~ MCQ of 7.8 represents the beginning of the second non-spontaneous step. The first non-spontaneous sorption step was denoted by distinct divergence of the negative $\Delta S^0$ and positive $\Delta H^0$ changes, both in the course toward infinity.

### 4.4. Adsorption kinetics modeling

Results of AMI adsorption on CR zeolite showed that intensive sorption occurred in the first 30 min of the process, when ~85% of the AMI was removed with regard to maximum ammonium ion uptake (Fig. 6). Dissolved AMI residue was adsorbed gradually, in the period of 100–120 min, until sorption equilibrium was reached. Obtained results confirm previously published adsorption kinetics data [69].

These adsorption rate changes in the beginning and the end of the process can be explained by the fact that all sorption active sites were free whereas groundwater AMI concentration was high. Number of active sites declined during the sorption process, and sorption rate decreased. Besides that, as a consequence of AMI concentration decrease, concentration gradient abated, and influenced on lesser sorption rate.

Pseudo-first and pseudo-second order kinetic constants calculated from the intercept and slope of linear plots of Eq. (23), and Eq. (24), respectively, are presented in Table 4.

Pseudo-second kinetic model showed better fitting to experimental data during analysis of linear coefficient correlation values. Also, differences between $q_e$ calculated and experimental values were lower when pseudo-second model was applied. The temperature increase had significant influence on initial rate and $k_2$ sorption rate values,

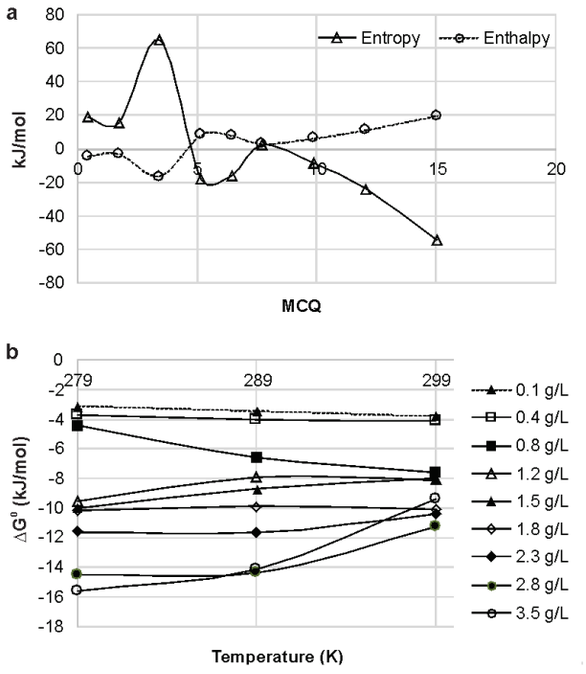


Fig. 5. Effect of zeolite concentration on: a) $\Delta H^0$ and $\Delta S^0$ changes; b) Gibbs free energy changes.

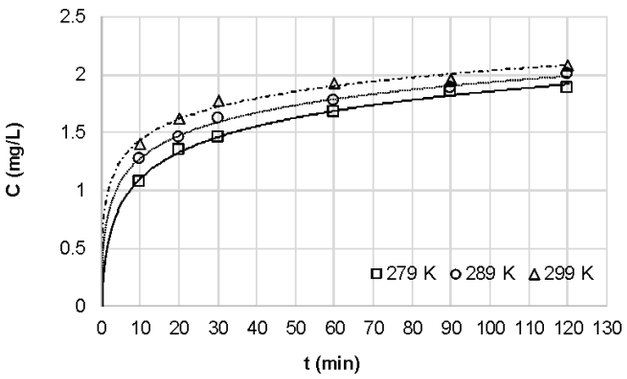


Fig. 6. Effect of contact time to adsorbed groundwater ammonium ion amount on zeolite CR-100.

and indicated more advantageous adsorption conditions at higher temperatures.

### 4.5. FTIR spectroscopy

FTIR spectrum of original CR zeolite (Fig. 7a) were performed for a qualitative comprehension of the CR composition, and it shows characteristic absorption peaks at 3,454 $cm^{-1}$, 1,640 $cm^{-1}$, and 1,030 $cm^{-1}$, that corresponds to –OH group (indicating the existence of the hydroxyl groups), lattice water, and ≡Si-O-Si≡ bonds, respectively. The peak around 445 $cm^{-1}$ is attributed to Al-O type bonds. FTIR spectra comparison of native CR (Fig. 7b curve 1) and CR after equilibrium with AMI at MCQ of 0.430 (Fig. 7b curve 2) indicating presence of adsorbed ammonium ions on the CR surface. An absorption band revealing the vibrational properties of ammonium group is visible around 1,460 $cm^{-1}$, as showed earlier [70]. These FTIR measurements found weak signal as consequence of small AMI amount adsorbed, additionally reduced due to dilution with KBr,

Table 4
Survey of sorption kinetics results modeling for ammonium ion adsorption on zeolite CR

| T (K) | | 279 | 289 | 299 |
|---|---|---|---|---|
| | | Pseudo-first model | | |
| $q_e$ (Model) | mg/g | 1.170 | 1.292 | 1.124 |
| $q_e$ (Exp) | mg/g | 1.912 | 2.011 | 2.102 |
| $k_1$ | g/mg·min | 0.031 | 0.035 | 0.028 |
| $R^2$ | | 0.990 | 0.885 | 0.928 |
| | | Pseudo-second model | | |
| $q_e$ (Model) | mg/g | 2.047 | 2.107 | 2.157 |
| $q_e$ (Exp) | mg/g | 1.912 | 2.011 | 2.102 |
| $k_2$ | g/mg·min | 0.391 | 0.506 | 0.712 |
| $h$ | mg/g·min | 0.191 | 0.240 | 0.330 |
| $R^2$ | | 0.999 | 0.998 | 0.999 |

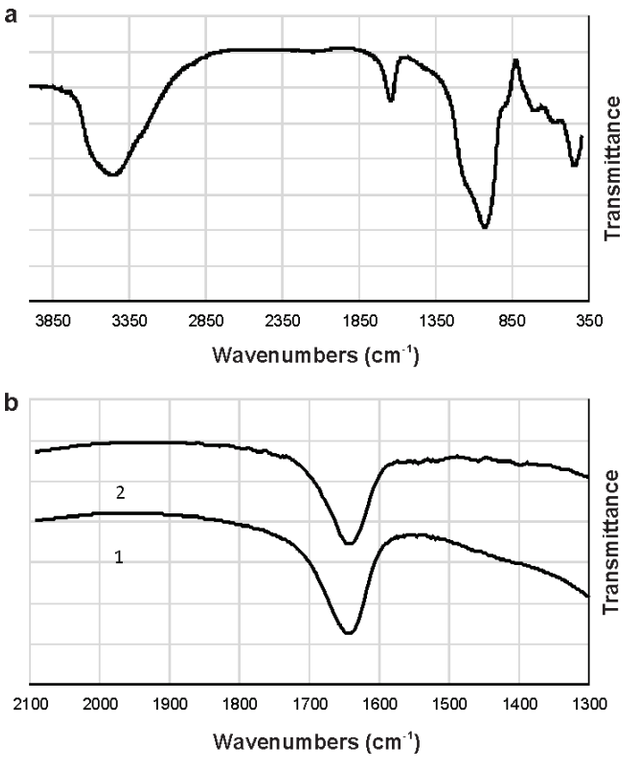


Fig. 7. Zeolite CR FTIR spectra of: a) Native CR bands; b) Zoomed CR spectra range (1) commercial zeolite, and (2) Appearance of adsorbed $NH_4^+$ bands.

and are used in order to confirm the formation of AMI on the surface of CR.

## 5. Conclusions

The sorption mechanism of natural groundwater ammonium ion through adsorption isotherms has proved as a three stage multilayer process. Higher temperatures induced more intensive multilayer bonding and sorption capacity increasing. AMI removal efficiency showed higher rate at lower MCQ and higher temperature. AMI sorption process onto zeolite CR showed absence of monolayer coverage only. Taking into account JIM constant values, existence of monolayer was indicative with low adsorption capacities decreased from lower to higher temperature, denoting exothermic adsorption. FIM and DRI adsorption capacities raised with temperature increase, indicating endothermic sorption process. This may be attributed to increased surface coverage at higher temperature, expansion and activation of reactive and bonding sites.

The highest coefficients of determination values of applied isotherm models were found for 289 K. Error analysis of theoretical and experimental nonlinear correlation indicated that the Freundlich model possessed the best fit. The shapes of experimental isotherms ensign that qe values corresponding to MCQ > 15, declined with the temperature raising, and opposite for the smaller MCQ values. These results indicated significant influence of temperature to AMI solubility different behavior in the identical sorption system.

Adsorption thermodynamic analysis has shown essential translation of most cardinal energetic values in the sense of sign changing during the investigated zeolite surface reactions. It is found that Crystal Right zeolite concentration, i.e. MCQ, played a crucial role in the changes of enthalpy, entropy and Gibbs free energy.

As adsorbent mass in the contact with solution less, adsorption is less spontaneous. These results were confirmed at the smallest CR concentrations. In this case low quantity of CR active sites were exposed to a huge quantity of ammonium species. Consequentially, enthalpy was negative and entropy positive, whereas Gibbs free energy achieved negative values near zero. Hence, low MCQ in the conditions of considerable high adsorbate content was extremely substantial to indicate ammonium species randomness and the degrees of freedom increase.

Molar ratio of zeolite to ammonium species quantity that was precedent to complete investigated sorption process should be defined dualistically. Sorption process was found to be slightly exothermic and spontaneous when MCQ was low, and exothermic and non-spontaneous in the conditions of high MCQ.

Obtained thermodynamic findings confirmed facts that increase of temperature at the high and low MCQ values decreased and increased adsorption capacities, respectively.

## References

[1] E.U. Council, Council Directive 98/83 EC on the Quality of Water Intended for Human Consumption, in, Official J. Eur. Commun., 1998.

[2] R. Boopathy, S. Karthikeyan, A.B. Mandal, G. Sekaran, Adsorption of ammonium ion by coconut shell-activated carbon from aqueous solution: kinetic, isotherm, and thermodynamic studies, Environ. Sci. Pollut. Res., 20 (2013) 533–542.

[3] N. Miladinovic, L.R. Weatherley, Intensification of ammonia removal in a combined ion-exchange and nitrification column, Chem. Eng. J., 135 (2008) 15–24.

[4] V.K. Gupta, H. Sadegh, M. Yari, R. Shahryari Ghoshekandi, B. Maazinejad, M. Chahardori, Removal of ammonium ions from wastewater: A short review in development of efficient methods, Global J. Environ. Sci. Manage., 1 (2015) 149–158.

[5] C.F. Hurtado, B. Cancino-Madariaga, Ammonia retention capacity of nanofiltration and reverse osmosis membranes in a non steady state system, to be use in recirculation aquaculture systems (RAS), Aquacult. Eng., 58 (2014) 29–34.

[6] H. Kurama, J. Poetzschke, R. Haseneder, The application of membrane filtration for the removal of ammonium ions from potable water, Water Res., 36 (2002) 2905–2909.

[7] H. Huang, X. Xiao, B. Yan, L. Yang, Ammonium removal from aqueous solutions by using natural Chinese (Chende) zeolite as adsorbent, J. Hazard. Mater., 175 (2010) 247–252.

[8] İ. Tosun, Ammonium removal from aqueous solutions by clinoptilolite: determination of isotherm and thermodynamic parameters and comparison of kinetics by the double exponential model and conventional kinetic models, Int. J. Environ. Res. Public Health, 9 (2012) 970–984.

[9] M. Turan, In: H. Ünlü, N.J.M. Horing, J. Dabrowski, Low-Dimensional and Nanostructured Materials and Devices: Properties, Synthesis, Characterization, Modelling and Applications, Springer International Publishing, Cham 2016, pp. 477–504.

[10] M. Franus, M. Wdowin, L. Bandura, W. Franus, Removal of environmental pollutions using zeolites from fly ash: A review, Fresen. Environ. Bull., 24 (2015) 854–866.

[11] J. Kyzioł-Komosińska, C. Rosik-Dulewska, M. Franus, P. Antoszczyszyn-Szpicka, J. Czupiol, I. Krzyzewska, Sorption capacities of natural and synthetic zeolites for Cu(II) Ions, Pol. J. Environ. Stud., 24 (2015) 1111–1123.

[12] A. Mittal, J. Mittal, A. Malviya, V.K. Gupta, Adsorptive removal of hazardous anionic dye "Congo red" from wastewater using waste materials and recovery by desorption, J. Colloid Interface Sci., 340 (2009) 16–26.

[13] V.K. Gupta, A. Nayak, Cadmium removal and recovery from aqueous solutions by novel adsorbents prepared from orange peel and $Fe_2O_3$ nanoparticles, Chem. Eng. J., 180 (2012) 81–90.

[14] N. Mohammadi, H. Khani, V.K. Gupta, E. Amereh, S. Agarwal, Adsorption process of methyl orange dye onto mesoporous carbon material–kinetic and thermodynamic studies, J. Colloid Interface Sci., 362 (2011) 457–462.

[15] V.K. Gupta, A. Mittal, D. Jhare, J. Mittal, Batch and bulk removal of hazardous colouring agent Rose Bengal by adsorption techniques using bottom ash as adsorbent, RSC Adv., 2 (2012) 8381–8389.

[16] Y.-S. Ho, W.-T. Chiu, C.-C. Wang, Regression analysis for the sorption isotherms of basic dyes on sugarcane dust, Bioresour. Technol., 96 (2005) 1285–1291.

[17] H.K. Boparai, M. Joseph, D.M. O'Carroll, Kinetics and thermodynamics of cadmium ion removal by adsorption onto nano zerovalent iron particles, J. Hazard. Mater., 186 (2011) 458–465.

[18] I. Mobasherpour, E. Salahi, M. Ebrahimi, Thermodynamics and kinetics of adsorption of Cu(II) from aqueous solutions onto multi-walled carbon nanotubes, J. Saudi Chem. Soc., 18 (2014) 792–801.

[19] H.R. Mahmoud, S.M. Ibrahim, S.A. El-Molla, Textile dye removal from aqueous solutions using cheap MgO nanomaterials: Adsorption kinetics, isotherm studies and thermodynamics, Adv. Powder Technol., 27 (2016) 223–231.

[20] S.P. Karthick, K.V. Radha, Equilibrium, isotherm, kinetic and thermodynamic adsorption studies of tetracycline hydrochloride onto commercial grade granular activated carbon, Int. J. Pharm. Pharm. Sci., 7 (2014) 42–51.

[21] V. Dulman, S.M. Cucu-Man, In: G. Crini, P.M. Badot, Sorption processes and pollution, Presses universitaires de Franche-Comté, University of Franche-Comté, 2009, pp. 233–267.
[22] B. Adane, K. Siraj, N. Meka, Kinetic, equilibrium and thermodynamic study of 2-chlorophenol adsorption onto Ricinus communis pericarp activated carbon from aqueous solutions, Green Chem. Lett. Rev., 8 (2015) 1–12.
[23] E. Mekonnen, M. Yitbarek, T.R. Soreta, Kinetic and thermodynamic studies of the adsorption of Cr(VI) onto some selected local adsorbents, S. Afr. J. Chem., 68 (2015) 45–52.
[24] S. Eturki, F. Ayari, N. Jedidi, H. Ben Dhia, Use of clay mineral to reduce ammonium from wastewater. Effect of various parameters, Surf. Eng. Appl. Elect., 48 (2012) 276–283.
[25] Y. Wimalasiri, M. Mossad, L. Zou, Thermodynamics and kinetics of adsorption of ammonium ions by graphene laminate electrodes in capacitive deionization, Desalination, 357 (2015) 178–188.
[26] D. Karadag, Y. Koc, M. Turan, B. Armagan, Removal of ammonium ion from aqueous solution using natural Turkish clinoptilolite, J. Hazard. Mater., 136 (2006) 604–609.
[27] A. Dąbrowski, Adsorption — from theory to practice, Adv. Colloid Interface Sci., 93 (2001) 135–224.
[28] A. Khosravi, M. Esmhosseini, S. Khezri, Removal of ammonium ion from aqueous solutions using natural zeolite: kinetic, equilibrium and thermodynamic studies, Res. Chem. Intermed., 40 (2014) 2905–2917.
[29] M.J. Kim, Effects of pH, adsorbate/adsorbent ratio, temperature and ionic strength on the adsorption of arsenate onto soil, Geochem.: Explor. Environ., Anal., 10 (2010) 407–412.
[30] A. Alshameri, C. Yan, Y. Al-Ani, A.S. Dawood, A. Ibrahim, C. Zhou, H. Wang, An investigation into the adsorption removal of ammonium by salt activated Chinese (Hulaodu) natural zeolite: Kinetics, isotherms, and thermodynamics, J. Taiwan Inst. Chem. E., 45 (2014) 554–564.
[31] M. Kukučka, N. Kukučka, M. Vojinović-Miloradov, Ž. Tomić, M. Šiljeg, A novel approach to determine a resin's sorption characteristics for the removal of natural organic matter and arsenic from groundwater, Water Sci. Technol., 11 (2011) 726–736.
[32] PuroTech Ltd., Installation, Operation & Maintenance Guide Crystal Right CR100 & CR200, 1–16.
[33] L. Lazar, B. Bandrabur, R.-E. Tataru-Fărmuş, M. Drobota, S.-G. Stroe, G. Gutt, Equlibrium Performances of Crystal-Right TM CR100 zeolite used in water softening process, Environ. Eng. Manag. J., 14 (2015) 541–549.
[34] Ž. Tomić, Possible application of synthetic zeolite CR-100 (Crystal-Right™) in ammonia adsorption from ground water of Banat aquifer, Faculty of Technology, Ph.D. thesis (2016) 134 pages.
[35] I. Langmuir, The constitution and fundamental properties of solids and liquids. Part I. Solids, J. Am. Chem. Soc., 38 (1916) 2221–2295.
[36] H.M.F. Freundlich, Uber die adsorption in losungen, Z. Phys. Chem, 57 (1906) 385–470.
[37] A.M.M. Vargas, A.L. Cazetta, M.H. Kunita, T.L. Silva, V.C. Almeida, Adsorption of methylene blue on activated carbon produced from flamboyant pods (Delonix regia): Study of adsorption isotherms and kinetic models, Chem. Eng. J., 168 (2011) 722–730.
[38] G.D. Halsey, The role of surface heterogeneity, Advances in Catalysis, 4 (1952) 259–269.
[39] M.J. Temkin, V. Pyzhev, Kinetics of ammonia synthesis on promoted iron catalysts, Acta Physiochim. Urss, 12 (1940) 217–222.
[40] M.M. Dubinin, L.V. Radushkevich, The equation of the characteristic curve of the activated charcoal, in: Proc. Acad. Sci. USSR Phys. Chem. Sect., Moscow, (1947), pp. 331–337.
[41] M. Hadi, M.R. Samarghandi, G. McKay, Equilibrium two-parameter isotherms of acid dyes sorption by activated carbons: Study of residual errors, Chem. Eng. J., 160 (2010) 408–416.
[42] S. Chowdhury, P. Saha, Adsorption thermodynamics and kinetics of Malachite Green onto $Ca(OH)_2$-Treated Fly Ash, J. Environ. Eng., 137 (2011) 388–397.
[43] P. Sampranpiboon, P. Charnkeitkong, X. Feng, Equilibrium isotherm models for adsorption of Zinc (II) ion from aqueous solution on pulp waste, WSEAS T. Environ. Develop., 10 (2014) 35–47.
[44] Z.A. Al-Anber, M.A.S. Al-Anber, Thermodynamics and kinetic studies of Iron (III) adsorption by olive cake in a batch system, J. Mex. Chem. Soc., 52 (2008) 108–115.
[45] F.-x. Chen, C.-r. Zhou, G.-p. Li, F.-f. Peng, Thermodynamics and kinetics of glyphosate adsorption on resin D301, Arab. J. Chem., 9 (2016) S1665–S1669.
[46] N.A. Oladoja, C.O. Aboluwoye, Y.B. Oladimeji, Kinetics and isotherm studies on Methylene Blue adsorption onto ground Palm Kernel Coat, Turk. J. Eng. Environ. Sci., 32 (2008) 303–312.
[47] R. Acosta, V. Fierro, A. Martinez de Yuso, D. Nabarlatz, A. Celzard, Tetracycline adsorption onto activated carbons produced by KOH activation of tyre pyrolysis char, Chemosphere, 149 (2016) 168–176.
[48] G. Hamscher, S. Sczesny, H. Hoper, H. Nau, Determination of persistent tetracycline residues in soil fertilized with liquid manure by high-performance liquid chromatography with electrospray ionization tandem mass spectrometry, Anal. Chem., 74 (2002) 1509–1518.
[49] S. Lagergren, Zur theorie der sogenannten adsorption gelöster stoffe. Kungliga Svenska Vetenskapsakademiens, Handlingar, 24 (1898) 1–39.
[50] K. Li, X. Wang, Adsorptive removal of Pb(II) by activated carbon prepared from Spartina alterniflora: Equilibrium, kinetics and thermodynamics, Bioresour. Technol., 100 (2009) 2810–2815.
[51] Y.S. Ho, G. McKay, Pseudo-second order model for sorption processes, Process Biochem., 34 (1999) 451–465.
[52] V.K. Gupta, I. Ali, Removal of endosulfan and methoxychlor from water on carbon slurry, Environ. Sci. Technol., 42 (2008) 766–770.
[53] Y.S. Ho, G. McKay, A comparison of chemisorption kinetic models applied to pollutant removal on various sorbents, Process Saf. Environ., 76 (1998) 332–340.
[54] A.E. Ofomaja, Y.-S. Ho, Equilibrium sorption of anionic dye from aqueous solution by palm kernel fibre as sorbent, Dyes Pigments, 74 (2007) 60–66.
[55] H. Zheng, L. Han, H. Ma, Y. Zheng, H. Zhang, D. Liu, S. Liang, Adsorption characteristics of ammonium ion by zeolite 13X, J. Hazard. Mater., 158 (2008) 577–584.
[56] S. Rani, D. Sud, Time and temperature dependent sorption behaviour of dimethoate pesticide in various Indian soils, Int. Agrophys., 28 (2014) 479.
[57] H. Zheng, D. Liu, Y. Zheng, S. Liang, Z. Liu, Sorption isotherm and kinetic modeling of aniline on Cr-bentonite, J. Hazard. Mater., 167 (2009) 141–147.
[58] J. Fraissard, C.W. Conner, Physical adsorption: Experiment, Theory and Applications, Kluwer Accademic Publishers, Dordrecht 1997.
[59] R. Leyva-Ramos, J.E. Monsivais-Rocha, A. Aragon-Piña, M.S. Berber-Mendoza, R.M. Guerrero-Coronado, P. Alonso-Davila, J. Mendoza-Barron, Removal of ammonium from aqueous solution by ion exchange on natural and modified chabazite, J. Environ. Manage., 91 (2010) 2662–2668.
[60] Q. Du, S. Liu, Z. Cao, Y. Wang, Ammonia removal from aqueous solution using natural Chinese clinoptilolite, Sep. Purif. Technol., 44 (2005) 229–234.
[61] M. Erşan, E. Bağda, E. Bağda, Investigation of kinetic and thermodynamic characteristics of removal of tetracycline with sponge like, tannin based cryogels, Colloid. Surface. B, 104 (2013) 75–82.
[62] A. Mittal, J. Mittal, A. Malviya, D. Kaur, V.K. Gupta, Decoloration treatment of a hazardous triarylmethane dye, Light Green SF (Yellowish) by waste material adsorbents, J. Colloid Interface Sci., 342 (2010) 518–527.

[63] Y. Yu, Y.-Y. Zhuang, Z.-H. Wang, Adsorption of water-soluble dye onto functionalized resin, J. Colloid Interface Sci., 242 (2001) 288–293.
[64] D. Saha, S. Deng, Characteristics of ammonia adsorption on activated alumina, J. Chem. Eng. Data, 55 (2010) 5587–5593.
[65] G.N. Manju, C. Raji, T.S. Anirudhan, Evaluation of coconut husk carbon for the removal of arsenic from water, Water Res., 32 (1998) 3062–3070.
[66] M. Uğurlu, M.H. Karaoğlu, Adsorption of ammonium from an aqueous solution by fly ash and sepiolite: Isotherm, kinetic and thermodynamic analysis, Microporous Mesoporous Mater., 139 (2011) 173–178.
[67] M. Kukučka, N. Kukučka, A. Kukučka, A novel approach to adsorption kinetics calculation, Microporous Mesoporous Mater., 228 (2016) 123–131.
[68] A. Mohseni-Bandpi, T.J. Al-Musawi, E. Ghahramani, M. Zarrabi, S. Mohebi, S.A. Vahed, Improvement of zeolite adsorption capacity for cephalexin by coating with magnetic $Fe_3O_4$ nanoparticles, J. Mol. Liq., 218 (2016) 615–624.
[69] F. Mazloomi, M. Jalali, Ammonium removal from aqueous solutions by natural Iranian zeolite in the presence of organic acids, cations and anions, J. Environ. Chem. Eng., 4 (2016) 240–249.
[70] F. Thibault-Starzyk, F. Maugé, In: M. Che, J.C. Védrine, Characterization of Solid Materials and Heterogeneous Catalysts: From Structure to Surface Reactivity, Wiley-VCH Verlag GmbH & Co. KGaA., 2012, pp. 15.